

Rab5 Mediates Caspase-8–promoted Cell Motility and Metastasis

Vicente A. Torres,^{*†} Ainhoa Mielgo,^{*†} Simone Barbero,^{*†} Ruth Hsiao,^{*†}
John A. Wilkins,[‡] and Dwayne G. Stupack^{*†}

^{*}Department of Pathology and [†]Moore's Comprehensive Cancer Center, University of California San Diego, School of Medicine, La Jolla, CA 92093; and [‡]Manitoba Centre for Proteomics and Systems Biology, University of Manitoba, Winnipeg, Manitoba, Canada R3E 3P4

Submitted September 8, 2009; Revised October 27, 2009; Accepted November 9, 2009
Monitoring Editor: Joan Brugge

Caspase-8 is a key apical sensory protein that governs cell responses to environmental cues, alternatively promoting apoptosis, proliferation, and cell migration. The proteins responsible for integration of these pathways, however, have remained elusive. Here, we reveal that Rab5 regulates caspase-8–dependent signaling from integrins. Integrin ligation leads to Rab5 activation, association with integrins, and activation of Rac, in a caspase-8–dependent manner. Rab5 activation promotes colocalization and coprecipitation of integrins with caspase-8, concomitant with Rab5 recruitment to integrin-rich regions such as focal adhesions and membrane ruffles. Moreover, caspase-8 expression promotes Rab5-mediated internalization and the recycling of $\beta 1$ integrins, increasing cell migration independently of caspase catalytic activity. Conversely, Rab5 knockdown prevented caspase-8–mediated integrin signaling for Rac activation, cell migration, and apoptotic signaling, respectively. Similarly, Rab5 was critical for caspase-8–driven cell migration *in vivo*, because knockdown of Rab5 compromised the ability of caspase-8 to promote metastasis under nonapoptotic conditions. These studies identify Rab5 as a key integrator of caspase-8–mediated signal transduction downstream of integrins, regulating cell survival and migration *in vivo* and *in vitro*.

INTRODUCTION

Cell migration is tightly controlled by the expression and localization of specific cell surface receptors, such as integrins; the remodeling of cytoskeleton elements, such as cortical actin; and the directed trafficking of molecules required for cell signaling and adhesion (Caswell and Norman, 2006; Pellinen and Ivaska, 2006; Palamidessi *et al.*, 2008). The relevance of the endosome trafficking machinery, and the Rab family of small GTPases in particular, in the regulation of these processes has become clear (Caswell and Norman, 2008). The Rab proteins are central regulators of endosome trafficking, and they are required for targeting, tethering, and transport of endosomes (Zerial and McBride, 2001; Markgraf *et al.*, 2007). Rab5 and Rab21 regulate early endosome dynamics, whereas Rab7 governs the transport of late endosomes. Rab4 acts as an early recycling regulator, whereas Rab11 also governs the “long” loop recycling from the perinuclear recycling compartment (Zerial and McBride, 2001).

Aside from endocytosis, Rabs can influence cell adhesion and migration (Caswell and Norman, 2006; Jones *et al.*, 2006; Caswell and Norman, 2008). On the one hand, Rab5 and Rab21 interact with $\beta 1$ integrins, regulating integrin trafficking (Pellinen *et al.*, 2006; Pellinen and Ivaska, 2006). On the other hand, Rab5 promotes lamellipodia formation (Spar-

garen and Bos, 1999) and actin reorganization after growth factor binding (Lanzetti *et al.*, 2004; Palamidessi *et al.*, 2008). This may occur via tyrosine kinase-mediated signaling to Rab5-GTPase activating proteins (GAPs) and Ras (Barbieri *et al.*, 2000; Lanzetti *et al.*, 2000; Lanzetti *et al.*, 2004). Accordingly, Rab5 regulation has been suggested to be important for understanding cancer cell motility (Tang and Ng, 2009).

Although a role for Rab5 in tumor cell migration was somewhat unexpected, focused studies over the past few years have identified many “unexpected” proteins that regulate cell motility. Caspase-8 is an apical protease that promotes apoptosis upon death receptor ligation, yet also promotes several nonapoptotic functions (Park *et al.*, 2005; Maelfait and Beyaert, 2008), including cell migration (Frisch, 2008). Many of the nonapoptotic functions of caspase-8 occur independently of its protease activity (Helfer *et al.*, 2006; Barbero *et al.*, 2008, 2009). Instead, caspase-8 can interact with several Src homology 2 domain-containing proteins, including the p85 α regulatory subunit of phosphatidylinositol 3-kinase (Senft *et al.*, 2007), Src family kinases (Barbero *et al.*, 2008; Finlay *et al.*, 2009), phosphatase SHP-1 (Jia *et al.*, 2008), and weakly with Grb2 (Barbero *et al.*, 2008). These interactions promote Rac and calpain activity (Helfer *et al.*, 2006; Senft *et al.*, 2007; Barbero *et al.*, 2009), as well as extracellular signal-regulated kinase signaling (Finlay and Vuori, 2007). Among cells with a compromised programmed cell death pathway, caspase-8 potentially promotes metastasis (Barbero *et al.*, 2009). Nonetheless, the precise mechanisms by which caspase-8 influences cell migration remain unclear.

We have shown that caspase-8 interaction with p85 α , a Rab5-GAP, alters Rab5-mediated endosome trafficking (Torres *et al.*, 2008). Because Rab5 regulates integrin trafficking and remodeling of the actin cytoskeleton, we hypothe-

This article was published online ahead of print in *MBC in Press* (<http://www.molbiolcell.org/cgi/doi/10.1091/mbc.E09-09-0769>) on November 18, 2009.

Address correspondence to: Dwayne G. Stupack (dstupack@ucsd.edu).

sized that Rab5 may act as a critical downstream effector of caspase-8. Here, we show that caspase-8-mediated activation of Rab5 is enhanced by integrin-mediated adhesion, which in turn alters integrin trafficking in tumor cells. Accordingly, we find that Rab5 is required for caspase-8-enhanced adhesion, migration, and metastasis under non-apoptotic conditions but promotes integrin-mediated death, an “active” mechanism of anoikis, when cells are deprived of integrin-mediated adhesion.

MATERIALS AND METHODS

Materials

Polyclonal anti-caspase-8 (catalog no. 559932) and monoclonal anti-caspase-8 (catalog no. 551242) antibodies were from BD Biosciences Pharmingen (San Diego, CA). Mouse monoclonal anti-Rab5 (catalog no. sc46692), rabbit polyclonal anti-Rab7 (catalog no. sc10767), rabbit polyclonal anti-Rab4 (catalog no. sc312), and goat polyclonal anti-Rab11 (catalog no. sc6565) antibodies were from Santa Cruz Biotechnology (Santa Cruz, CA). Mouse monoclonal anti-Rab21 (H00023011-M01) was from Novus Biologicals (Littleton, CO). Polyclonal anti-early endosomal antigen (EEA1) (catalog no. ab50313) and polyclonal anti-M6PR (catalog no. ab32815) antibodies were from Abcam (Cambridge, MA). Goat anti-rabbit and goat anti-mouse antibodies coupled to horseradish peroxidase and monoclonal anti-actin antibody (catalog no. A5316) were from Bio-Rad Laboratories (Hercules, CA). Alexa Fluor488- and Alexa Fluor568-labeled secondary antibodies and Geneticin (G418 sulfate, catalog no. 11811) were from Invitrogen (Carlsbad, CA). Cell medium and antibiotics were from Cellgro Mediatech (Herdon, VA). Fetal bovine serum (FBS; catalog no. SH30070.03) was from HyClone Laboratories (Logan, UT). The peroxidase substrate 2,2'-azino-bis(3-ethylbenzthiazoline-6-sulfonic acid) was from Sigma-Aldrich (St. Louis, MO). Glutathione-Sepharose 4B was from GE Healthcare (Piscataway, NJ). The chemiluminescent substrate (catalog no. 34078) and protein A/G beads were from Pierce Chemical (Rockford, IL). Protease inhibitors cocktail tablets were from Roche Diagnostics (Mannheim, Germany). Caspase-8 and Rab5 lentiviral short hairpin RNAs (shRNA) were from Open Biosystems (Huntsville, AL).

Cell Culture

A549 cells were cultured in DMEM supplemented with 10% FBS and antibiotics (10,000 U/ml penicillin and 10 µg/ml streptomycin) at 37°C, 5% CO₂. Neuroblastoma cells NB7 and NB7C8 were cultured in RPMI 1640 medium with 10% FBS and antibiotics, as described previously. Caspase-8 was knocked down in A549 cells by stable lentiviral delivery of shRNA as described previously (Torres *et al.*, 2008). Control cells were infected with a lentivirus encoding a nonspecific shRNA sequence (plasmid 1864; Addgene, Cambridge, MA). Rab5 down-regulation in A549 and neuroblastoma NB7 and NB7C8 cells was similarly performed by stable delivery of lentiviral shRNA (catalog no. RHS3979-98491128; Open Biosystems). Stably transfected cells were selected and maintained in presence of 400 µg/ml puromycin.

Immunofluorescence

Cells were grown by 24 h on glass coverslips, either uncoated or precoated with 2 µg/ml fibronectin (Sigma-Aldrich), and subjected to analysis, as indicated. After rinsing with phosphate-buffered saline (PBS), cells were fixed in PBS/4% paraformaldehyde (10 min), permeabilized with 0.1% Triton X-100 (5 min), and blocked with 2% bovine serum albumin in PBS (30 min) at room temperature. Samples were then incubated with either monoclonal anti-Rab5 immunoglobulin G (IgG) (1:50), polyclonal anti-Rab5 IgG (1:50), or a cocktail of monoclonal anti-β1 (B44, JB1, and JB1A, 3 µg/ml each) primary antibodies, followed by incubation with the respective Alexa Fluor-conjugated secondary antibodies (1:250). Nuclei were stained with TO-PRO-3 (1:500) (Invitrogen). Samples were then washed and mounted onto slides with the Vectashield hard-set mounting media (Vector Laboratories, Burlingame, CA) and visualized on an Eclipse C1 confocal microscope (Nikon, Melville, NY), with a 1.4 numerical aperture 60× oil immersion lens, by using minimum pinhole (30 µm). Images were captured using EZ-C1 3.50 imaging software. For colocalization analysis, ImageJ software (National Institutes of Health, Bethesda, MD) was used. First, both red and green channels to be analyzed were adjusted to 160 pixels, and the integrated intensity of pixels for each channel was measured. The integrated intensity of pixels colocalized was measured by using the “Colocalization RGB Plugin” of Image J. Colocalized pixels were normalized against total intensity of pixels of β1 integrin, and data are expressed as percentage of colocalization.

Western Blotting

For whole cell extracts, cells were lysed in radioimmunoprecipitation assay (RIPA) buffer (100 mM Tris base, 150 mM NaCl, 1 mM EDTA, 1% deoxycholic acid, 1% Triton X-100, 0.1% SDS, and 50 mM NaF) containing protease

inhibitors, boiled in Laemmli buffer, and separated by SDS-polyacrylamide gel electrophoresis (PAGE) on 10 or 12% acrylamide minigels (Bio-Rad Laboratories), by loading 25 µg of total protein per lane and then transferred to nitrocellulose. Blots were blocked with 5% milk in 0.1% Tween-PBS and then probed with anti-actin (1:5000), anti-caspase-8 (1:1000), anti-Rab5 (1:500), anti-Rab7 (1:300), anti-β1 (JB1A, 1:1000), anti-Rab21 (1:500), or anti-Rac1 (1:500) antibodies. Bound antibodies were detected with horseradish peroxidase-conjugated secondary antibodies and the enhanced chemiluminescence system.

Immunoprecipitation

Cell extracts were prepared in a buffer containing 20 mM Tris, pH 7.4, 150 mM NaCl, 1% NP-40, and protease inhibitors by 5-min incubation on ice. Samples were centrifuged at 13,000 × g by 1 min at 4°C, and postnuclear supernatants (500 µg total protein) were immunoprecipitated with protein A/G bead-immobilized antibodies by 30 min. β1 was immunoprecipitated with 10 µg of a rabbit polyclonal antibody (catalog no. 664; Millipore Bioscience Research Reagents, Temecula, CA) and Rab5 was immunoprecipitated with 5 µg of a mouse monoclonal antibody (mAb). Immunoprecipitated samples were solubilized in Laemmli buffer, boiled and separated by SDS-PAGE, and analyzed by Western blotting as indicated above.

Pull-Down Assays for Guanosine Triphosphate (GTP)-loaded Rab5 and Rac

Cells were allowed to attach onto fibronectin coated plates (2 µg/ml) by 1 h and subsequently lysed in a buffer containing 25 mM HEPES, pH 7.4, 100 mM NaCl, 5 mM MgCl₂, 1% NP-40, 10% glycerol, 1 mM dithiothreitol, and protease inhibitors. Extracts were incubated by 5 min on ice and clarified by centrifugation (10,000 × g for 1 min at 4°C). Postnuclear supernatants were used immediately for pull-down assays, by adding 100 µl of precoated beads. Glutathione-beads precoating with 100 µg of glutathione transferase (GST)-R5BD (Torres *et al.*, 2008) or 50 µg of GST-PAK1 (generously donated by Dr. Gary Bokoch of the Scripps Research Institute; Knaus *et al.*, 2007) was performed by 1 h at 4°C in a rotating shaker. Pull-down incubations were carried out by 15 min in a rotating shaker at 4°C. Thereafter, beads were collected, washed three times with lysis buffer containing 0.01% NP-40 and protease inhibitors. Samples were boiled in Laemmli buffer and separated by SDS-PAGE and analyzed by Western blotting as indicated above.

Endosome Fractionation in Sucrose Gradients

Endosome fractionation was performed as described previously by ultracentrifugation in discontinuous sucrose gradients (Gorvel *et al.*, 1991; Torres *et al.*, 2008). Late and early endosome fractions (45 µl each) were analyzed by Western blotting against β1 integrin. Fraction purity was controlled by both Western blotting against EEA1 (early endosomes) and Rab7 (late endosomes) and by tracking the relative accumulation of endocytosed horseradish peroxidase, which was measured by incubation with the substrate 2,2'-azino-bis(3-ethylbenzthiazoline-6-sulfonic acid).

Internalization and Recycling Assays

Integrin internalization and recycling assays were performed as described previously (Roberts *et al.*, 2001). For internalization assays, cells were labeled with 0.2 mg/ml sulfosuccinimidyl 2-(biotinamido)-ethyl-1,3-dithiopropanoate (NHS-SS-biotin) by 30 min at 4°C, washed, and brought to 37°C in serum-free medium containing 0.6 µM primaquine. Incubations were allowed at different times and stopped on ice. Residual surface NHS-SS-biotin was removed with 20 mM MESNA and quenched with 20 mM iodoacetamide. Then, cell extracts were obtained and internalized biotinylated β1 level measured by immunoprecipitating β1 integrin, Western blotting, and scanning densitometry. For recycling experiments, internalization was allowed by 30 min, and then surface biotin was removed with 20 mM MESNA (Sigma-Aldrich) and the samples were incubated at different times in serum-free medium 37°C. Incubations were stopped on ice and recycled biotin was removed with MESNA and quenched with iodoacetamide. Biotinylated β1 was measured as indicated above. Alternatively, β1 biotinylation was confirmed in capture enzyme-linked immunosorbent assay, by using P4C10-precoated plates (5 µg/ml).

Wound-healing Assay

Twelve-well plates were coated overnight with 5 µg/ml fibronectin in PBS at 4°C. Cells were allowed to attach by 2 h at confluence (500,000 cells/well), and then monolayers were wounded twice with a conditioned p200 pipette tip. Wounds were allowed to close by 20 h and subsequently, wound areas were recorded under the microscope. Wound areas were measured in Photoshop CS2 (Adobe Systems, Mountain View, CA). Four regions per well were recorded, with a total of four wells per condition. Data were averaged from three independent experiments.

Transwell Migration Assay

Assays were performed in modified Boyden Chambers Transwell Costar (Corning Life Sciences, Lowell, MA) (6.5 mm in diameter; 8 µm pore size),

according to the manufacturer's protocol. In brief, the bottom sides of the inserts were coated with 2 $\mu\text{g}/\text{ml}$ fibronectin. Cells (1×10^5) were plated in the top chamber of Transwell inserts, and serum-free medium was added to the bottom chamber. After 2 h, stationary cells were removed from the top side of the membrane, whereas migrated cells in the bottom side of the inserts were stained with 0.1% crystal violet in 2% ethanol. Dye was eluted with methanol, and absorbance was measured at 600 nm.

Adhesion Assay

Cells were brought in suspension in serum-free medium and allowed to attach onto fibronectin-coated 24-well plates (2 $\mu\text{g}/\text{ml}$) at different times as indicated. Nonadherent cells were removed by gentle wash in serum free medium and adherent cells were stained with 0.1% crystal violet in 2% ethanol. Dye was eluted with methanol, and absorbance was measured at 600 nm.

Preparation of Focal Adhesion-enriched Fractions

Fractionation was performed as described previously (Barbero *et al.*, 2009). In brief, cells were plated onto fibronectin-coated plates (2 $\mu\text{g}/\text{ml}$) and allowed to attach by 45 min. Adherent cells were pre-extracted with lysis buffer containing 0.5% Triton X-100 by 30 min at 4°C, and the fraction was clarified by centrifugation (500 $\times g$ for 5 min) to remove nuclei; this fraction is referred to as "cytosolic fraction." The remaining cell fraction attached to the plate was extracted with RIPA buffer for 5 min on ice and scraped off the plates. Fractions were clarified by centrifugation at 14000 $\times g$ for 10 min. This fraction is referred to as "focal adhesion-enriched fraction." Both cytosolic and focal adhesion fractions were analyzed by Western blotting.

Surface $\beta 1$ Integrin Analysis

Cells were grown for 24 h at subconfluence in complete medium. Thereafter, cells were brought in suspension and blocked in 0.5% FBS/PBS for 30 min at 4°C. Cells were then incubated with the monoclonal antibodies P4C10 (total $\beta 1$) or B44 (active $\beta 1$) in the presence or absence of 500 μM MnCl_2 by 60 min at 4°C, followed by a 45 min incubation with APC-conjugated goat anti-mouse IgG. Finally, cells were resuspended in PBS and analyzed by flow cytometry (FACSCalibur; BD Biosciences, Mountain View, CA) by using the CellQuest program.

Chick Chorioallantoic Membrane Tumor Growth and Metastasis Assay

This assay was performed as described previously (Stupack *et al.*, 2006). In brief, neuroblastoma cells (5×10^6) were suspended in 40 μl of complete medium and seeded onto the chorioallantoic membrane of 11-d-old chicks. Tumors were left to develop for 8 d and then resected and weighed. Lung and bone marrow metastases were assessed by amplification of human-specific Alu sequences as reported previously.

Statistical Analysis

Where pertinent, results were compared using noncorrected or Welch-corrected unpaired *t* tests by using InStat 3 software (GraphPad Software, San Diego, CA). Unless indicated, at least three independent experiments were subjected to statistics. A *p* value <0.05 was considered significant.

RESULTS

Caspase-8 Regulates Rab5 Activation and Association with $\beta 1$ Integrin Complexes

Caspase-8 regulates endosome trafficking via effects on the subcellular targeting and activation of the small GTPase Rab5 (Torres *et al.*, 2008). As Rab5 signaling has been linked to processes promoted by caspase-8, including apoptosis, cell adhesion, migration, and cytoskeletal remodeling, we evaluated whether Rab5 was also a key effector of these activities. On adhesion to fibronectin substrate, we found that neuroblastoma cells lacking caspase-8 showed no increase in Rab5 activation, whereas those reconstituted for caspase-8 expression showed robust activation of Rab5 (Figure 1A). Increasing levels of active Rab5 were observed upon adhesion in a time-dependent manner (Supplemental Figure 1A). This process was initiated by integrin-mediated engagement of the underlying substrate because this process was mimicked by attachment to substrate-immobilized $\beta 1$ integrin-specific antibodies (P4C10) but not by interactions with control antibody (anti-CD44)-coated surfaces (Figure 1B).

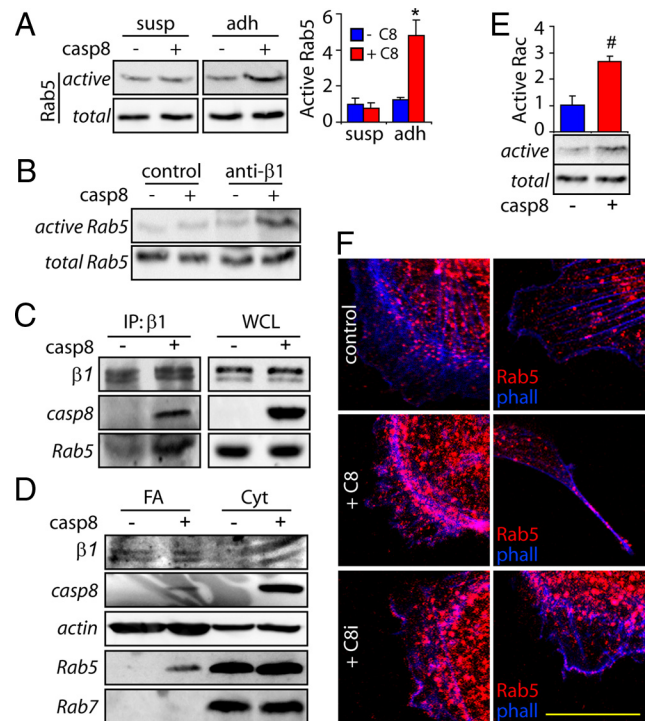


Figure 1. Caspase-8 regulates Rab5 activation and association with $\beta 1$ integrin. (A) Rab5-GTP loading assays were performed on NB7 neuroblastoma cells deficient for (–), or reconstituted with (+) caspase-8, that were either held in suspension (susp) or allowed to attach to fibronectin substrates (2 $\mu\text{g}/\text{ml}$) for 45 min (adh). Representative immunoblots as well as a quantification of three independent experiments is shown (mean \pm SE; **p* < 0.05). (B) Neuroblastoma cells, as described above, were allowed to attach onto plates coated with 10 $\mu\text{g}/\text{ml}$ anti- $\beta 1$ integrin or anti CD44 mAb (control, 10 $\mu\text{g}/\text{ml}$) for 45 min. Rab5 GTP levels were measured as indicated in A. One of two similar experiments is shown. (C) $\beta 1$ integrin and associated complex was immunoprecipitated from the neuroblastoma cell lines. Rab5, caspase-8, and integrin were detected by immunoblotting in both immunoprecipitates (IP) and whole cell lysates. (D) Isolated focal adhesion (FA) and cytosolic (Cyt) fractions were analyzed by immunoblotting with caspase-8, actin, Rab5, and Rab7 antibodies, as shown. Data are representative of three independent experiments. (E) Quantification of Rac activation after cellular attachment to fibronectin coated plates (2 $\mu\text{g}/\text{ml}$); extracts were obtained and Rac-GTP levels were measured as indicated in A, by using a GST-PAK1 pull-down assay. Data shown are averaged from three independent experiments (mean \pm SE; #*p* < 0.01). (F) Neuroblastoma cells stably expressing GFP (control), GFP-caspase-8 (C8), or GFP-caspase 8/C360A (C8i) were grown on glass coverslips, fixed, and analyzed by confocal microscopy. Rab5 (red channel) and actin (phalloidin, blue channel) staining are shown. Bar, 10 μm .

This integrin and caspase-8-dependent activation of Rab5 prompted us to further test how these three proteins were functionally related. Because Rab5 was shown previously to associate with integrins (Pellinen *et al.*, 2006), we evaluated whether caspase-8 expression influenced this interaction. As reported previously (Pellinen *et al.*, 2006), Rab5 coprecipitated in a complex with $\beta 1$; however, the extent of coprecipitation was dramatically increased among cells expressing caspase-8 (Figure 1C). As expected, caspase-8 was also detected in the precipitated complex (Stupack *et al.*, 2001; Figure 1C). To further determine whether caspase-8 promoted Rab5 recruitment specifically to integrin-containing adhesion complexes, we evaluated the presence of these proteins in isolated focal adhesion fractions (Barbero *et al.*,

2009). As observed in the coprecipitation studies, caspase-8 and Rab5, but not Rab7, were detected in focal adhesion fractions of caspase-8-expressing, but not caspase-8-deficient neuroblastoma cells (Figure 1D). Together, these results indicate that integrin ligation promotes caspase-8-dependent activation and relocalization of Rab5.

Rab5 activity was required for association with integrin because the GTPase-deficient mutant Q79L, but not the guanosine diphosphate (GDP)-bound S34N variant, was found to coprecipitate with integrins (Supplemental Figure 2, A and B). Conversely, Rab5 activation increased formation of a complex between caspase-8 and $\beta 1$ integrins as observed by immunoprecipitation (Supplemental Figure 2C) and colocalization studies (Supplemental Figure 2, D and E).

In agreement with previous studies (Helfer *et al.*, 2006), caspase-8 enhanced Rac activity after integrin ligation (Figure 1E and Supplemental Figure 1B), which suggested a regulatory role at the leading lamella. Because Rab5 localizes to the cell periphery after caspase-8 expression (Torres *et al.*, 2008), we next characterized the role of Rab5 at the leading lamella. Immunofluorescence colocalization studies revealed that Rab5 was enriched in punctate structures that localized adjacent to membrane ruffles of caspase-8-expressing cells (Figure 1F). This did not require caspase-8 proteolytic activity, as a catalytic-deficient mutant of caspase-8 (C360A) recapitulated this phenotype (Figure 1F, bottom), confirming that proteolysis is dispensable to effect Rab5 localization (Torres *et al.*, 2008). Importantly, green fluorescent protein (GFP)-tagged wild-type caspase-8 or the C360A mutant of caspase-8, but not GFP alone, colocalized with Rab5 at membrane ruffles (Barbero *et al.*, 2008; data not shown). Interestingly, expression of caspase-8 did not impart detectable changes in Rab5 and $\beta 1$ colocalization within the body of the cell. Rather, caspase-8 expression was associated with increased recruitment and colocalization of Rab5 with $\beta 1$ at the cell periphery (Figure 2, A and B).

Caspase-8 Expression Alters Integrin Trafficking

Rab5-integrin colocalization in punctate vesicle-like structures suggested association during endosomal sorting and/or recycling. Overall, integrin accumulation within endosome fractions was increased among cells expressing caspase-8, and there was a selective and modest decrease in integrins within late endosomes (Figure 2C), although immunofluorescence studies suggested minimal integrin within late endosomes in general (data not shown). In contrast, we saw no differences in total $\beta 1$ integrins, or in active conformers, by fluorescence-activated cell sorting assessment of caspase-8-expressing or -deficient cells (Figure 2D), nor were there differences in total $\beta 1$ by immunoblot analysis (data not shown).

Nonetheless, dynamic studies of integrin trafficking revealed much higher rates of internalization among caspase-8-expressing cells, with initial rates approximately three- to fourfold higher than caspase-8-deficient cells. However, the overall capacity of the caspase-8-deficient cells to internalize integrin, given enough time (~ 15 – 20 min), was similar to those expressing caspase-8. Accordingly, the rate of surface recycling of integrins was slightly accelerated among cells expressing caspase-8 (Figure 2E). Together, these results raised the notion that caspase-8 may influence the rate of integrin traffic to and from remodeling adhesion complexes via activation of Rab5.

Rab5 Is Required for Caspase-8-imparted Cell Motility

The expression of caspase-8 in neuroblastoma cells enhances cell migration (Helfer *et al.*, 2006; Barbero *et al.*, 2009).

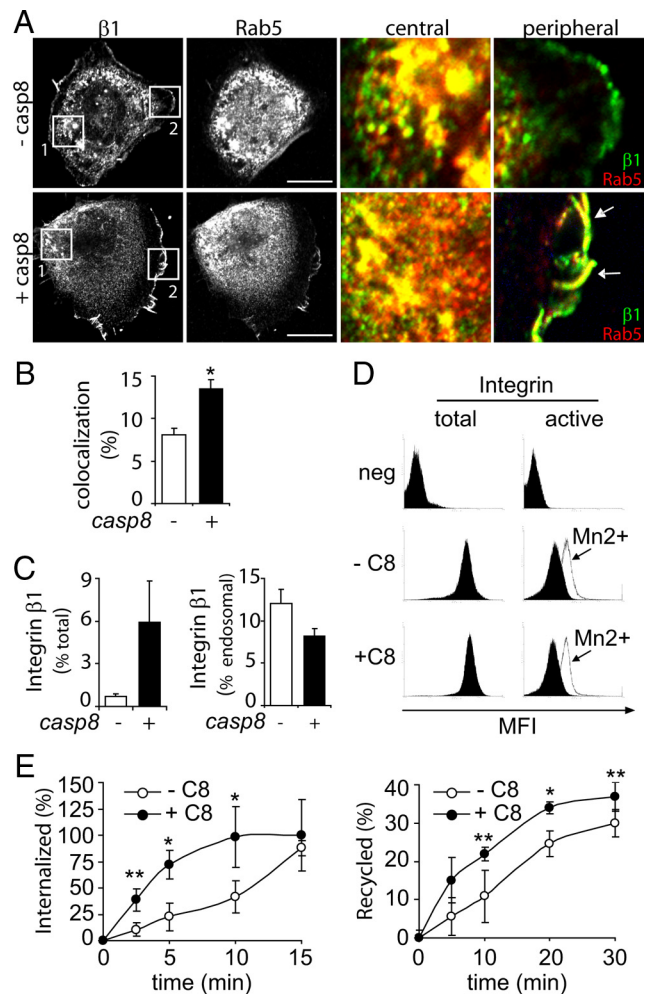


Figure 2. Caspase-8-dependent regulation of $\beta 1$ integrin trafficking. (A) NB7 neuroblastoma cells lacking ($-$ casp8) or expressing caspase-8 ($+$ casp8) were permitted to attach to fibronectin coated coverslips ($2 \mu\text{g}/\text{ml}$) for 60 min, fixed, and confocal analysis of Rab5 (red channel) and $\beta 1$ integrin (green channel) was performed. A representative image from three independent experiments is shown. The right panels denote magnified regions from pictures on left: the perinuclear region ("central") and the cell edge ("peripheral"). Bar, $10 \mu\text{m}$. (B) Colocalization analysis of Rab5 and integrin was performed with ImageJ software (as described in *Materials and Methods*); the mean of three experiments \pm SE is shown; $*p < 0.01$. (C) Neuroblastoma cells lacking ($-$) or expressing ($+$) caspase-8 were fractionated on discontinuous sucrose gradients, and integrin distribution in early or late endosome fractions quantified by immunoblotting and scanning densitometry. Integrin detected in the total pool of endosomes is shown in the left graph as percentage of total integrin in whole cell lysates; integrin associated with late endosomes fractions is shown in the right graph as percentage of total pool of endosomes (mean of three experiments \pm SE). (D) Neuroblastoma cells lacking ($-$ C8) or expressing caspase 8 ($+$ C8) were analyzed by flow cytometry for expression of total integrin (left) or active integrin conformers (right) alone or in the presence of 200 mM MnCl_2 (open histograms) to "activate" integrin. (E) Internalization and recycling of $\beta 1$ integrin were measured in NB7 cells lacking ($-$ C8) or reconstituted for caspase 8 ($+$ C8) expression. For internalization studies (left), cells were labeled with $0.2 \text{ mg}/\text{ml}$ NHS-SS-biotin for 30 min at 4°C , washed, and then brought to 37°C in serum-free medium; cell extracts were obtained and biotinylated integrin measured by immunoprecipitation, immunolotting, and scanning densitometry. Recycling experiments (right) permitted internalization for 30 min, and then surface biotin was removed and samples incubated at times as shown in serum-free medium 37°C . Data are shown as the mean \pm SE of three experiments ($*p < 0.05$; $**p < 0.1$).

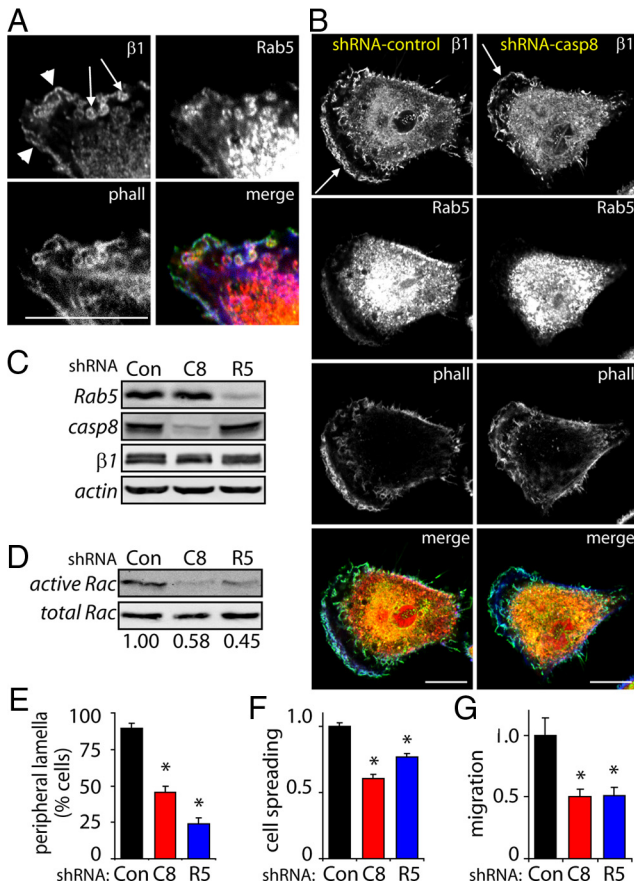


Figure 3. Requirement of caspase-8 and Rab5 for A549 cell migration. (A) A549 cells were allowed to attach and spread onto fibronectin-coated coverslips (2 $\mu\text{g}/\text{ml}$) for 60 min, fixed, and analyzed by confocal microscopy for the presence of Rab5 (red channel), $\beta 1$ integrin (green channel), and actin (phalloidin; blue channel). (B) A549 cells treated with control (left) or caspase-8-targeted (right) shRNA were attached to fibronectin and stained for Rab5, $\beta 1$ integrin, and actin, as indicated above. Bar, 10 μm . (C) Rab5, caspase-8, and $\beta 1$ integrin levels were assessed by immunoblot analysis of A549 cell lysates, by using lines expressing the control, caspase-8-, or Rab5-targeted shRNAs, as indicated. (D) Cells treated with control (Con), caspase-8- (C8), or Rab5 (R5)-targeted shRNA were attached to fibronectin-coated plates (2 $\mu\text{g}/\text{ml}$) by 45 min, and extracts were obtained. Rac-GTP levels were measured as indicated in Figure 1A, by using the GST-PAK1 pull-down assay. Numbers indicate averages from two independent experiments. (E) Ruffle quantification in A549 cells stably expressing control (Con), caspase-8- (C8), or Rab5-targeted (R5) shRNAs. Cells were allowed to attach to fibronectin substrates for 60 min, fixed, and analyzed by phalloidin staining. The percentage of cells with peripheral ruffles is shown (data from two independent experiments, $n = 25$ images; * $p < 0.001$ relative to control). (F) Cells attached to fibronectin-coated coverslips and analyzed by confocal microscopy, as in (A). Cell area was measured via NIH-Image J software, and cell area shown normalized to cells treated with control shRNA. Data were averaged from 25 pictures (mean \pm SE). * $p < 0.005$ relative to control. (G) Cell migration was evaluated in Transwell plates coated with fibronectin (2 $\mu\text{g}/\text{ml}$) for 2 h, as indicated in the *Materials and Methods*, and data are normalized to controls. Data shown are from two independent experiments done in triplicate (mean \pm SE). * $p < 0.01$ relative to control.

Caspase-8 enhanced migration is a common event among tumor cell lines, and thus, perhaps not surprisingly, suppression of caspase-8 expression in A549 lung carcinoma cells decreased overall migration (see text below and Figure 3). Rab5 was readily detected at membrane ruffles colocaliz-

ing with integrin in control or parental A549 cells (Figure 3A); however, this localization was disrupted among caspase-8 knockdown cells (Figure 3, B and C).

A549 cells form characteristic circular ruffles that are indicative of a Rab5-mediated Rac activation (Palamidessi *et al.*, 2008; arrows in Figure 3A), and accordingly, Rac activation was readily detected in A549 cells attached to a fibronectin substrate (Figure 3D). However, shRNA-mediated knockdown of either caspase-8 or Rab5 abrogated Rac activation after cell adhesion to fibronectin (Figure 3, C and D). Similarly, the appearance of lamella, a hallmark indicator of Rac activation, was reduced among cells in which either caspase-8 or Rab5 expression were knocked down (Figure 3E). Accordingly, suppression of caspase-8 or Rab5 compromised cell spreading (Figure 3F), as well as migration in a Boyden chamber assay (Figure 3G).

Neuroblastoma cells do not form ruffles as readily as A549 cells, although peripheral ruffling can be observed (Figure 1; data not shown). This can be enhanced by observing cells in directed migration, such as in a wound-closing assay (Barbero *et al.*, 2008). Assessing the localization of Rab5 in neuroblastoma cells expressing GFP-tagged caspase-8 (or control GFP), we found that Rab5, integrins, and caspase-8 were selectively colocalized at the leading lamella of cells invading the wound (Figure 4A).

Caspase-8 promotes neuroblastoma cell migration independent of caspase-8 catalytic activity (Helfer *et al.*, 2006; Barbero *et al.*, 2009). The requirement of Rab5 in caspase-8-driven cell migration was evaluated by comparing control cells with those bearing an shRNA-mediated knockdown of caspase-8 (Figure 4B). Although the accelerated integrin trafficking observed in caspase-8-expressing cells (Figure 2E) was compromised by Rab5 knockdown (Supplemental Figure 3A), no other changes in surface (Supplemental Figure 3B), endosomal (Supplemental Figure 3C), or total integrin levels (Figure 4B) were observed, nor were there differences in related Rabs, such as Rab21 (Figure 4B). However, knockdown of Rab5 suppressed caspase-8-enhanced adhesion (Figure 4C), Rac activation (Figure 4D), and cell migration (Figure 4E). Similarly, Rab5 knockdown impaired caspase-8-dependent cell migration in a wound-healing assay (Figure 4, F and G). The difference in wound closure did not seem to be solely due to a delay in initiating cell migration because both the Rab5-deficient and -competent cells began migrating into the wound within one hour. However, although Rab5/caspase-8-competent cells closed wounds within 18–20 h, cells deficient in either Rab5 or caspase-8 typically required >30 h, consistent with a change in cellular migration rate (Helfer *et al.*, 2006). Changes in cell migration by caspase-8 and Rab5 seemed to be specific for integrins, rather than a general phenomenon because no differences were observed in migration mediated by other surface molecules, such as CD44, whose surface expression remained unaffected upon caspase-8 or Rab5 expression (Supplemental Figure 4; data not shown).

Notably, among cells invading a matrix which is inappropriate to their integrin complement, caspase-8 promotes apoptosis in an integrin-dependent manner (Stupack *et al.*, 2001). Similar to caspase-8-enhanced migration, Rab5 knockdown also compromised this integrin-mediated event (Supplemental Figure 3). Together, these data indicate that Rab5 is a key regulator of signals from the local microenvironment, acting cooperatively with caspase-8 to regulate cell invasion.

Caspase-8-enhanced Metastasis Is Rab5 Dependent

Among cells with compromised apoptotic pathways, caspase-8 expression can enhance tumor metastasis (Barbero *et al.*,

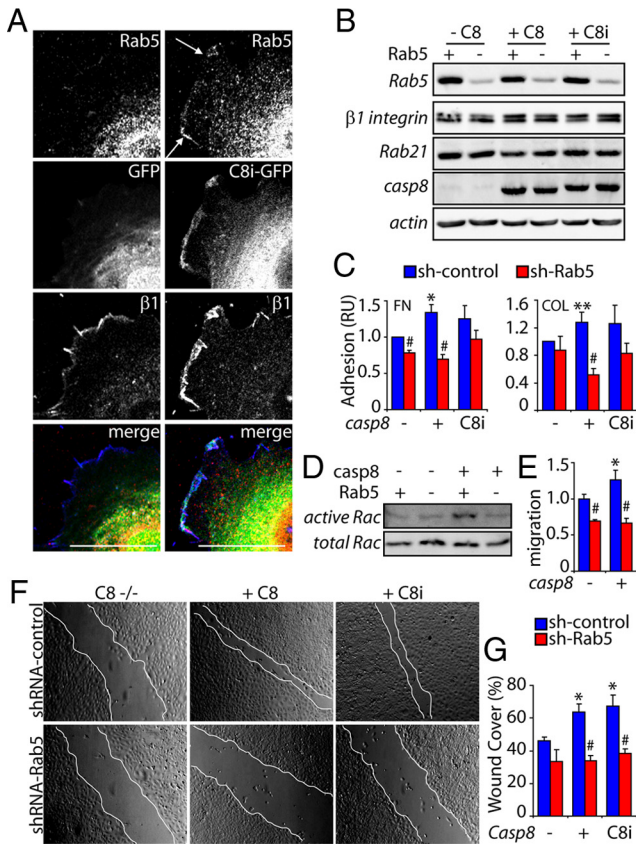


Figure 4. Caspase-8–driven neuroblastoma cell adhesion and migration require Rab5. (A) NB7 cells stably expressing GFP (left) or GFP-caspase-8(C360A) (C8i-GFP, right) were plated at confluence on 2 $\mu\text{g}/\text{ml}$ fibronectin-coated coverslips, the monolayer wounded, and cells allowed to migrate into the wound for 4 h. Cells were then fixed and stained for Rab5 (polyclonal antibody; red channel) and integrin $\beta 1$ (blue channel). Bar, 10 μm . (B) NB7 cells deficient (–C8) or reconstituted for caspase 8 (+C8) or a mutant caspase 8 (C360A, ‘C8i’) and coexpressing either control (+) or Rab5 shRNA (–), as indicated, were lysed and assessed by immunoblotting for their relative expression of Rab5, Rab21, $\beta 1$ integrin, caspase-8, and actin. (C) Cells, as described above, were permitted to attach to fibronectin- (2 $\mu\text{g}/\text{ml}$) or collagen (10 $\mu\text{g}/\text{ml}$)-coated substrates for 30 min, and the observed adhesion was normalized to controls. The mean \pm SE of three experiments is shown (* $p < 0.01$, ** $p < 0.05$, compared with casp8–; # $p < 0.01$, compared with shRNA-control). (D) Cells treated with control (+) or Rab5 shRNA (–), either lacking (–) or expressing caspase 8 (+) were permitted to attach to fibronectin-coated plates (2 $\mu\text{g}/\text{ml}$), and Rac-GTP levels were measured (as per Figure 1A) after 45 min. (E) Cell migration was assessed in Transwell chambers plates coated with fibronectin (2 $\mu\text{g}/\text{ml}$) after 2 h. Data are normalized to control cells, and representative of two independent experiments done in triplicate (mean \pm SE). * $p < 0.05$, compared with casp8–; # $p < 0.01$, compared with shRNA-control. (F and G) shRNA control or shRNA Rab5-treated cells, either lacking (–) or expressing caspase 8 (+) or caspase 8/C360A (C8i) were allowed to attach onto fibronectin (2 $\mu\text{g}/\text{ml}$) at confluence. The monolayer was wounded, and cells were allowed to migrate for 16 h. (F) Representative phase contrast images are shown. (G) Quantification of three independent experiments each performed in triplicate. Data represent the mean \pm SE; * $p < 0.05$, compared with casp8–; # $p < 0.01$, relative to shRNA control.

2009), whereas among cells with intact apoptotic pathways, caspase-8 acts as a metastasis suppressor, promoting apoptosis among cells invading an ‘‘inappropriate’’ tumor environment (Stupack *et al.*, 2006). Given the key role of Rab5

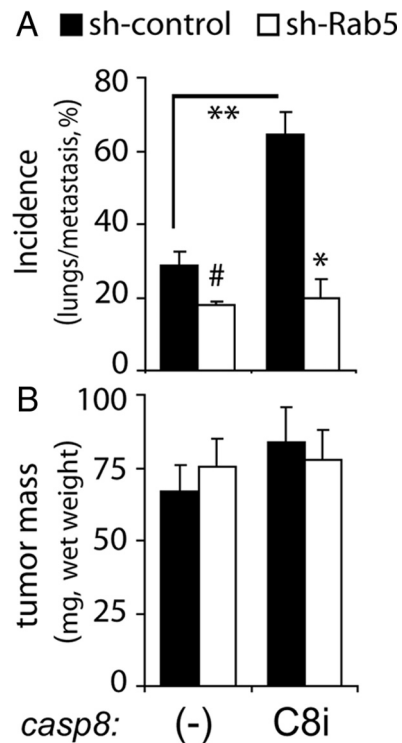


Figure 5. Caspase-8 enhances neuroblastoma metastasis under nonapoptotic conditions in a Rab5-dependent manner. Control shRNA (black bars) or Rab5-shRNA–treated cells (open bars) either lacking (–) or expressing caspase 8/C360A (C8i) were seeded into the upper chorioallantoic membrane of 10-d-old chick embryos, and tumors were permitted to develop for 8 d. (A) Total cumulative incidence of detected human Alu sequences, (expresses as percentage) from genomic DNA isolated from lungs of the tumor-seeded chick cohorts was measured by polymerase chain reaction. Statistical comparisons between cohorts representing three experiments were done via unpaired *t* test. (# $p = 0.30$; ** $p = 0.09$; * $p = 0.07$). (B) Tumors were resected from the chorioallantoic membrane, and the wet weight was determined (mean \pm SE).

expression in caspase-8–enhanced invasiveness after integrin ligation, we hypothesized that Rab5 might be critical for metastasis in vivo. To test this possibility, tumors were grown on the chorioallantoic membrane of 10-day-old chick embryos, and lung metastasis were assessed 8 d later, as described previously (Stupack *et al.*, 2006). Because wild-type caspase-8 promotes apoptosis in neuroblastoma cells, we tested the C360A mutant, which recapitulates the proinvasive phenotypes but will not trigger cell death. In agreement with a previous report (Barbero *et al.*, 2009), the expression of ‘‘nonapoptotic’’ caspase-8 increased tumor metastasis compared with cells lacking caspase-8 (Figure 5A). Rab5 down-regulation did not affect basal metastasis of cells lacking caspase-8, but it significantly decreased metastasis induced by caspase-8 (Figure 5A). Importantly, tumor size remained unaffected under these conditions (Figure 5B). Together, these results identify an integrin–caspase-8–Rab5 axis, which promotes cell invasion in vitro and in vivo.

DISCUSSION

This study has focused on understanding the molecular effectors for caspase-8–potentiated extracellular matrix (ECM) attachment and migration. Although integrin expres-

sion and activation remained unaltered following caspase-8 expression, $\beta 1$ integrin trafficking was increased. This required Rab5 activation and recruitment to caspase-8 and integrin-containing complexes, including focal adhesions (Barbero *et al.*, 2009). Immunoprecipitation, subcellular fractionation, and immunofluorescence studies supported the notion that caspase-8 promotes Rab5 association with $\beta 1$ integrin complexes. Indeed, both proteins were found to colocalize within endosomes and membrane ruffles. Rab5 binding proteins, such as p120RasGAP, are known to be peripherally or implicitly associated with focal adhesion complexes (Liu and Li, 1998) and integrins (Meng *et al.*, 2004). Supporting this, preliminary total internal reflection fluorescence microscopy examinations of Rab5 and $\beta 1$ localization show increased membrane localization (data not shown) in a caspase-8-dependent manner.

Both wild type and a constitutively active Rab5 (Q79L), but not an inactive GDP-bound Rab5 (S34N), associated with integrins (Supplemental Figure 1), paralleling observations with the related protein Rab21 (Pellinen *et al.*, 2006). Rab21 can also regulate integrin trafficking, cell adhesion, and migration (Pellinen *et al.*, 2006), although in our system we observed no changes in Rab21 levels after expression or down-regulation of caspase-8 or Rab5, suggesting that the events described in our tumor cell models are Rab5 specific. Similarly, the endosome-recycling GTPases Rab4 (short loop) and Rab11 (perinuclear recycling compartment, long loop) (Caswell and Norman, 2006) were unaffected by caspase-8 expression in terms of localization and expression (data not shown), suggesting that Rab5 is a relatively specific effector of caspase-8 and integrin signaling. However, it remains unclear whether the function of any of these Rabs, which act downstream of Rab5, are altered in response to caspase-8 expression.

It has been suggested that association of Rac with the Rac-GEF Tiam1 after growth factor treatment occurs within early endosomes and involves a clathrin- and Rab5-dependent mechanism that is a requisite for Rac activation. This allows the specific delivery of active Rac to those subcellular locations where it is required for signaling and actin remodeling (Lanzetti *et al.*, 2004; Palamidessi *et al.*, 2008). We observed substantial caspase-8-dependent Rac activation in our tumor cell models, in agreement with studies from the Frisch laboratory (Helfer *et al.*, 2006). Rab5 was critical for this regulation, as Rab5 depletion compromised integrin-caspase-8-mediated Rac activation (Figure 4D). Rac and Rab5 dictate the morphology and motility mode of tumor cells, and promote movement via "mesenchymal-type" motility mechanisms (Palamidessi *et al.*, 2008). Accordingly, suppression of Rab5 expression also compromised caspase-8-promoted metastasis (Figure 5).

ECM attachment via integrins promoted Rab5 activation selectively among cells that express caspase-8 (Figure 1, A and B). The first phase of signaling following integrin ligation seems to occur via nonreceptor tyrosine kinases of the Src and focal adhesion kinase family kinases (Mittra and Schlaepfer, 2006). Tyrosine phosphorylation of caspase-8 may promote compartmentalization of Rab-GAP activity (Torres *et al.*, 2008), leading to activation of Rab5 targets, such as the endosomal Rac1-GEF Tiam 1, or may promote more direct effects, such Rab5 association with the focal adhesion complex proteins, such as integrin (Pellinen *et al.*, 2006) or RasGAP (Liu and Li, 1998). Caspase-8 and integrins associate in a complex whether integrins are unligated (Stupack *et al.*, 2001, 2006) or ligated (Barbero *et al.*, 2009). The interactions are biosensory and direct cell behavior in response to the local extracellular milieu. Nonetheless,

the precise determinants that regulate the process have remained elusive. Here, our work reveals integrins, caspase-8 and Rab5 to function collaboratively and to associate in a precipitable, functionally codependent molecular complex, and in particular, Rab5 functions as a key effector of caspase-8 signaling.

ACKNOWLEDGMENTS

We thank Dr. Sandra Schmid for insightful discussions, intellectual input, and careful review of this work. This work was supported by National Cancer Institute/National Institutes of Health grant CA-107263 (to D. S.).

REFERENCES

- Barbero, S., Barila, D., Mielgo, A., Stagni, V., Clair, K., and Stupack, D. (2008). Identification of a critical tyrosine residue in caspase 8 that promotes cell migration. *J. Biol. Chem.* 283, 13031–13034.
- Barbero, S., *et al.* (2009). Caspase-8 association with the focal adhesion complex promotes tumor cell migration and metastasis. *Cancer Res.* 69, 3755–3763.
- Barbieri, M. A., Roberts, R. L., Gumusboga, A., Highfield, H., Alvarez-Dominguez, C., Wells, A., and Stahl, P. D. (2000). Epidermal growth factor and membrane trafficking. EGF receptor activation of endocytosis requires Rab5a. *J. Cell Biol.* 151, 539–550.
- Caswell, P., and Norman, J. (2008). Endocytic transport of integrins during cell migration and invasion. *Trends Cell Biol.* 18, 257–263.
- Caswell, P. T., and Norman, J. C. (2006). Integrin trafficking and the control of cell migration. *Traffic* 7, 14–21.
- Finlay, D., Howes, A., and Vuori, K. (2009). Critical role for caspase-8 in epidermal growth factor signaling. *Cancer Res.* 69, 5023–5029.
- Finlay, D., and Vuori, K. (2007). Novel noncatalytic role for caspase-8 in promoting SRC-mediated adhesion and Erk signaling in neuroblastoma cells. *Cancer Res.* 67, 11704–11711.
- Frisch, S. M. (2008). Caspase-8, fly or die. *Cancer Res.* 68, 4491–4493.
- Gorvel, J. P., Chavrier, P., Zerial, M., and Gruenberg, J. (1991). rab5 controls early endosome fusion in vitro. *Cell* 64, 915–925.
- Helfer, B., *et al.* (2006). Caspase-8 promotes cell motility and calpain activity under nonapoptotic conditions. *Cancer Res.* 66, 4273–4278.
- Jia, S. H., Parodo, J., Kapus, A., Rotstein, O. D., and Marshall, J. C. (2008). Dynamic regulation of neutrophil survival through tyrosine phosphorylation or dephosphorylation of caspase-8. *J. Biol. Chem.* 283, 5402–5413.
- Jones, M. C., Caswell, P. T., and Norman, J. C. (2006). Endocytic recycling pathways: emerging regulators of cell migration. *Curr. Opin. Cell Biol.* 18, 549–557.
- Knaus, U. G., Bamberg, A., and Bokoch, G. M. (2007). Rac and Rap GTPase activation assays. *Methods Mol. Biol.* 412, 59–67.
- Lanzetti, L., Palamidessi, A., Areces, L., Scita, G., and Di Fiore, P. P. (2004). Rab5 is a signalling GTPase involved in actin remodelling by receptor tyrosine kinases. *Nature* 429, 309–314.
- Lanzetti, L., Rybin, V., Malabarba, M. G., Christoforidis, S., Scita, G., Zerial, M., and Di Fiore, P. P. (2000). The Eps8 protein coordinates EGF receptor signalling through Rac and trafficking through Rab5. *Nature* 408, 374–377.
- Liu, K., and Li, G. (1998). Catalytic domain of the p120 Ras GAP binds to RAB5 and stimulates its GTPase activity. *J. Biol. Chem.* 273, 10087–10090.
- Maelfait, J., and Beyaert, R. (2008). Non-apoptotic functions of caspase-8. *Biochem. Pharmacol.* 76, 1365–1373.
- Markgraf, D. F., Peplowska, K., and Ungermann, C. (2007). Rab cascades and tethering factors in the endomembrane system. *FEBS Lett.* 581, 2125–2130.
- Meng, X., Krishnan, J., She, Y., Ens, W., Standing, K., and Wilkins, J. A. (2004). Association of rasgap SH3 binding protein 1, G3BP1, and rasCap120 with integrin containing complexes induced by an adhesion blocking antibody. *J. Proteome Res.* 3, 506–516.
- Mittra, S. K., and Schlaepfer, D. D. (2006). Integrin-regulated FAK-Src signaling in normal and cancer cells. *Curr. Opin. Cell Biol.* 18, 516–523.
- Palamidessi, A., Frittoli, E., Garre, M., Faretta, M., Mione, M., Testa, I., Diaspro, A., Lanzetti, L., Scita, G., and Di Fiore, P. P. (2008). Endocytic trafficking of Rac is required for the spatial restriction of signaling in cell migration. *Cell* 134, 135–147.

- Park, S. M., Schickel, R., and Peter, M. E. (2005). Nonapoptotic functions of FADD-binding death receptors and their signaling molecules. *Curr. Opin. Cell Biol.* *17*, 610–616.
- Pellinen, T., Arjonen, A., Vuoriluoto, K., Kallio, K., Fransen, J. A., and Ivaska, J. (2006). Small GTPase Rab21 regulates cell adhesion and controls endosomal traffic of beta1-integrins. *J. Cell Biol.* *173*, 767–780.
- Pellinen, T., and Ivaska, J. (2006). Integrin traffic. *J. Cell Sci.* *119*, 3723–3731.
- Roberts, M., Barry, S., Woods, A., van der Sluijs, P., and Norman, J. (2001). PDGF-regulated rab4-dependent recycling of alphavbeta3 integrin from early endosomes is necessary for cell adhesion and spreading. *Curr. Biol.* *11*, 1392–1402.
- Senft, J., Helfer, B., and Frisch, S. M. (2007). Caspase-8 interacts with the p85 subunit of phosphatidylinositol 3-kinase to regulate cell adhesion and motility. *Cancer Res.* *67*, 11505–11509.
- Spaargaren, M., and Bos, J. L. (1999). Rab5 induces Rac-independent lamellipodia formation and cell migration. *Mol. Biol. Cell* *10*, 3239–3250.
- Stupack, D. G., Puente, X. S., Boutsaboualoy, S., Storgard, C. M., and Cheresch, D. A. (2001). Apoptosis of adherent cells by recruitment of caspase-8 to unligated integrins. *J. Cell Biol.* *155*, 459–470.
- Stupack, D. G., Teitz, T., Potter, M. D., Mikolon, D., Houghton, P. J., Kidd, V. J., Lahti, J. M., and Cheresch, D. A. (2006). Potentiation of neuroblastoma metastasis by loss of caspase-8. *Nature* *439*, 95–99.
- Tang, B. L., and Ng, E. L. (2009). Rabs and cancer cell motility. *Cell Motil. Cytoskeleton* *66*, 365–370.
- Torres, V. A., Mielgo, A., Barila, D., Anderson, D. H., and Stupack, D. (2008). Caspase 8 promotes peripheral localization and activation of Rab5. *J. Biol. Chem.* *283*, 36280–36289.
- Zerial, M., and McBride, H. (2001). Rab proteins as membrane organizers. *Nat. Rev. Mol. Cell Biol.* *2*, 107–117.